Differential dependency of human glioblastoma cells on vascular endothelial growth factor-A signaling via neuropilin-1

JUNGWHOI LEE[1*], KYUHA CHONG[2-4*], JUNGSUL LEE[5], CHUNGYEUL KIM[6], JAE-HOON KIM[1], KYUNGSUN CHOI[7] and CHULHEE CHOI[5,7]

[1]Department of Applied Life Science, Sustainable Agriculture Research Institute (SARI), Jeju National University, Jeju-do 63243; [2]Department of Neurosurgery, Korea University Guro Hospital, Korea University Medicine, Korea University College of Medicine, Guro-gu, Seoul 08308; [3]Laboratory of Photo-Theranosis and Bioinformatics for Tumors, Department of Neurosurgery, Samsung Medical Center; [4]Department of Neurosurgery, Brain Tumor Center, Samsung Medical Center, Sungkyunkwan University School of Medicine, Gangnam-gu, Seoul 06351; [5]Department of Bio and Brain Engineering, KAIST, Yuseong-gu, Daejeon 34141; [6]Department of Pathology, Korea University Guro Hospital, Korea University Medicine, Korea University College of Medicine, Guro-gu, Seoul 08308; [7]ILIAS Biologics Inc., Yuseong-gu, Daejeon 34014, Republic of Korea

Received February 27, 2022; Accepted July 22, 2022

DOI: 10.3892/ijo.2022.5412

Abstract. Despite the high expression of neuropilin-1 (NRP-1) in human glioblastoma (GB), the understanding of its function as a co-receptor of vascular endothelial growth factor receptors (VEGFRs) in angiogenesis is currently limited. Therefore, the aim of the present study was to elucidate the non-classical function of NRP-1 expression in human GB. Expression patterns of NRP-1 and VEGF-A were determined by sandwich ELISA, western blot analysis, or immunohistochemistry. Differential dependency of GB cells following ablation of VEGF-A signaling was validated *in vitro* and *in vivo*. Cellular mechanism responsible for distinct response to VEGF-A signaling was evaluated by western blotting and immunoprecipitation analysis. Prognostic implications were assessed using IHC analysis. GB cells exhibited differing sensitivity to silencing of vascular endothelial growth factor (VEGF)-A signaling, which resulted in a distinct expression pattern of wild-type or chondroitin-sulfated NRP-1. VEGF-A-sensitive GB exhibited the physical interaction between wild-type NRP-1 and FMS related receptor tyrosine kinase 1 (Flt-1) whereas VEGF-A-resistant GB exhibited chondroitin-sulfated NRP-1 without interaction with Flt-1. Eliminating the chondroitin sulfate modification in NRP-1 led to re-sensitization to VEGF-A signaling, and chondroitin sulfate modification was found to be associated with an adverse prognosis in patients with GB. The present study identified the distinct functions of NRP-1 in VEGF-A signaling in accordance with its unique expression type and interaction with Flt-1. The present research is expected to provide a strong basis for targeting VEGF-A signaling in patients with GB, with variable responses.

Correspondence to: Dr Jungwhoi Lee, Department of Applied Life Science, Sustainable Agriculture Research Institute (SARI), Jeju National University, 102 Jeju Daehak-ro, Jeju-do 63243, Republic of Korea
E-mail: sdjd1108@kaist.ac.kr

Dr Chulhee Choi, ILIAS Biologics Inc., 40-20 Techno 6-ro, Yuseong-gu, Daejeon 34014, Republic of Korea, Republic of Korea
E-mail: cchoi@iliasbio.com

*Contributed equally

Key words: neuropilin-1, glioblastoma, chondroitin sulfate, FMS related receptor tyrosine kinase 1, autocrine signaling

Introduction

Glioblastoma (GB) is the most common and fatal brain tumor, as it involves a grave prognosis (1). According to the World Health Organization (WHO) classification, GB is designated as grade IV astrocytoma either generated anew (primary GB) or recrudesced from a residual low-grade tumor (secondary GB) (2-4). GB is characterized by rapid cell proliferation, infiltrative migration, and aggressive invasion into adjacent brain parenchyma. Although existing research has developed progressive surgical resection accompanied by numerous tryout therapies, the mean survival time of patients with GB is still <1 year from diagnosis (5-7).

Neuropilin-1 (NRP-1) is a cell surface co-receptor of vascular endothelial growth factor (VEGF)-A_{165} with fetal liver kinase 1 (Flk-1) in endothelial cells that is mainly recognized for its function in the development of blood vessels (8,9). Recent studies have revealed that NRP-1 is highly expressed in various types of cancers, including GB, and stimulates malignancy (10-13). NRP-1 plays a critical role in tumor development by activating tumor angiogenesis (14,15). It has also been suggested that NRP-1 can be modified by adding glycosaminoglycan (GAG) chains in endothelial cells and various cancer cells (13,16). GAGs are fundamental

components of proteoglycans and the extracellular matrix (ECM) that contribute to the regulation of cell proliferation, differentiation, and paracrine cell-matrix interaction, and its chondroitin-sulfated modification or derestriction is correlated with clinical outcomes in various malignant tumors (17,18). Although sporadic studies, as aforementioned, have presented the expression patterns of NRP-1, the biological significance of NRP-1 expression pattern in malignant GB remains ambiguous.

In a previous study by the authors it was reported that various malignant tumors including GB have differing sensitivities to VEGF-A signaling (19). The aim of the present study was to further investigate the mechanism responsible for the differential dependency of GB to VEGF-A signaling and create an effective strategy for the blockade of GB via silencing of VEGF-A signaling.

Materials and methods

Overview. To investigate the association between differential dependency of VEGF-A signaling and NRP-1 expression type in GB cells, experimental verifications such as *in vitro*, *in vivo*, and patient sample analyses were performed. For the experimental preparation, a number of GB cell lines and a human primary astrocyte cell line were used. To elucidate the expression pattern of NRP-1 and its association with sensitivity to VEGF-A signaling in GB cells, *in vitro* and *in vivo* experiments were performed such as proliferation assays, si-RNA transfection against Flt-1, Flk-1, NRP-1 and VEGF-A, sandwich enzyme-linked immunosorbent assay (ELISA), western blot analysis, immunoprecipitation, immunohistochemistry, and a xenograft model. To verify the association between chondroitin-sulfated NRP-1 expression and insensitivity to VEGF-A signaling in GB cells, chondroitinase ABC (Ch-ABC) was used *in vitro* and *in vivo*. To confirm clinical significance, immunohistochemical analysis using a tissue microarray study of patients with GB was designed and the association between chondroitin sulfate expression and prognosis of patients with GB was verified by a pathologist blinded to the sample identities.

Gene expression analysis. The microarray expression profiles were obtained from the public microarray database Gene Expression Omnibus (GEO) at NCBI (https://www.ncbi.nlm.nih.gov/geo/) in the previously described manner (20). A total of four datasets were used including GSE16011 (21), GSE4290 (22), GSE4271 (23), and GSE2727. All data were normalized by Robust Multichip Average (RMA) method (21). BrainArray probe annotation was used, and the values of several probes for one gene were averaged into a value for the gene as previously described (22). The statistical significance of the differences in each expression was assessed using the Student's t-test, where unequal variance was assumed if the P-value of one-way ANOVA was <0.05, and where equal variance was assumed otherwise.

Cell culture and reagents. U251-MG, U373-MG, CRT-MG, and LN215-MG cells were kindly provided by Professor Etty N. Benvenite (University of Alabama, Birmingham, USA) and the human primary astrocytes were kindly provided by Professor In-Hong Choi (Yonsei University, Seoul, Korea). The human primary astrocytes were prepared according to a previously described procedure (23). The human umbilical vein endothelial cells (HUVECs; CRL-1730) were purchased from ATCC. A172 (KCLB no. 21620), SNU-466 (KCLB no. 00466), SNU-489 (KCLB no. 00489), SNU-626 (KCLB no. 00626), and SNU-1105 (KCLB no. 01105) were obtained from the Korean Cell Line Bank (KCLB). LN215-MG and U251-MG cells were grown in DMEM (Gibco-BRL; Thermo Fisher Scientific, Inc.) and A172, CRT-MG, SNU-466, SNU-489, SNU-626, SNU-1105, and U373-MG cells were grown in RPMI-1640 medium (Gibco-BRL; Thermo Fisher Scientific, Inc.) supplemented with 10% fetal bovine serum (Gibco-BRL; Thermo Fisher Scientific, Inc.) and penicillin-streptomycin 100 mg/l (Invitrogen; Thermo Fisher Scientific, Inc.) at 37˚C in a humidified atmosphere containing 5 % CO_2. HUVECs were grown in EGM-2 Bulletkit medium (Lonza Group, Ltd.) at 37˚C in a humidified atmosphere containing 5% CO_2. All experiments were performed using HUVECs within 3-7 passages. U373-MG cells were authenticated using short tandem repeat (STR) analysis by Macrogen, Inc. Antibodies of Flk-1 (cat. no. sc-6251) and Flt-1 (cat. no. sc-271789) were obtained from Santa Cruz Biotechnology, Inc. Phosphorylated (p)-FAK (Y397; cat. no. 8556), FAK (cat. no. 71433), p-AKT (Ser473; cat. no. 4060), AKT (cat. no. 9272), NRP-1 (cat. no. 3725), caspase-3 (cat. no. 9662), cleaved caspase-3 (cat. no. 9664), and glyceraldehyde 3-phosphate dehydrogenase (GAPDH; cat. no. 5174) were purchased from Cell Signaling Technology Inc. 4G10 (cat. no. 05-321), anti-phosphotyrosine antibody, and p-Flt-1 (Y1213; #07-758) were obtained from MilliporeSigma. SU1498 (cat. no. SML1193), a VEGFR inhibitor, and Ch-ABC (cat. no. SAE0150) were purchased from Sigma-Aldrich; Merck KGaA. Recombinant VEGF-A (cat. no. 293-VE) was obtained from R&D Systems Inc.

Small interfering RNA (siRNA) transfection. Transfection of siRNAs was performed using Effectene® transfection reagent (Qiagen GmbH), in U251-MG, U373-MG, LN215-MG, and SNU-466 cells as previously described (24,25). The siRNA oligonucleotides (100 pmole/μl) that encode VEGF-A, Flt-1, Flk-1, NRP-1, and scrambled control were obtained from Bioneer Corporation (Daejeon, Korea). The sequences of the siRNAs were as follows: VEGF-A, 5'-AAAUGUGAAUGCAGACCAA-3'-dTdT; FLT-1; 5'-GACUCUCUUCUGGCUCCUA-3'-dTdT; FLK-1, 5'-CUCCUAAUGAGAGUUCCUU-3'-dTdT; NRP-1, 5'-GUCCGAAUCAAGCCUGCAA-3'-dTdT; and scrambled control, 5'-CCUACGCCAAUUUCGU-3'-dTdT. U251-MG, U373-MG, LN215-MG, and SNU-466 cells ($1x10^5$ cells/well) were seeded in six-well plates (Nunc S/A; Nalge Nunc International), and after 18 h, transfection was performed with 2 μl si-RNAs or scrambled si-RNA and 208 μl Effectene reagent (200 μl of buffer; 3 μl of enhancer; 5 μl of Effectene) in a final volume of 2,500 μl RPMI-1640 medium containing 10% serum without antibiotics. The cells were then maintained an additional 72 h at 37˚C in a humidified incubator containing 5% CO_2. The efficacy of siRNA transfection was confirmed by western blot analysis of the corresponding proteins.

Assessment of cell death. To evaluate cell viability for the treatment of exogenous VEGF-A and SU1498, WST-1 reagent (cat. no. 89-024-504; Nalgene; Thermo Fisher Scientific, Inc.) was used as previously described (25). After 30 min of incubation at room temperature, the absorbance was measured at 450 nm using a microplate reader (Bio-Rad Laboratories, Inc.). To assess cell death for the combination treatment of SU1498 and Ch-ABC, lactate dehydrogenase (LDH) assay (cat. no. J2380; Promega Corporation) was conducted according to the manufacturer's protocol.

Western blot analysis. To evaluate Flt-1, Flk-1, and NRP-1 expression in nine GB cell lines and human primary astrocytes, western blotting was performed as previously described (25). For whole cell lysates, cells were lysed in M-PER lysis buffer (cat. no. 78501; Thermo Fisher Scientific, Inc.) containing protease and phosphatase inhibitors. The total quantity of protein was determined with BCA Protein Assay kit (cat. no. 23227; Thermo Fisher Scientific, Inc.). Cell lysates (20 μg) were separated by 10% sodium dodecyl sulfate-polyacrylamide gel electrophoresis and transferred onto a nitrocellulose membrane (cat. no. 10600003; Amersham Biosciences; Cytiva). The membrane was blocked using 5% (w/v) bovine serum albumin and 0.2% (v/v) Tween-20 in Tris-buffered saline (T-TBS) for 2 h at room temperature and then incubated with diluted antibodies (1:2,000 specific for NRP-1 or 1:1,000 for Flt-1 and Flk-1), overnight at 4˚C. After each incubation with primary antibodies, the membranes were washed three times with T-TBS buffer for 10 min each prior to incubation with 1:5,000 secondary antibody (goat-anti rabbit IgG-HRP, cat. no. sc-2004 for NRP-1; goat-anti mouse IgG-HRP, cat. no. sc-2005 for Flt-1 and Flk-1; Santa Cruz Biotechnology, Inc.) for 1 h at room temperature. To visualize bands on an X-ray film, SuperSignal West Pico PLUS Chemiluminescent Substrate (cat. no. 34580; Thermo Fisher Scientific, Inc.) was used. Bands were assessed by densitometric analysis using ImageJ software (ver. 1.46r; National Institutes of Health). To ensure equal protein loading, GAPDH was used as the reference.

ELISA. The Human VEGF Duoset® ELISA Development System (cat. no. DY293B; R&D Systems, Inc.) was used with cultured supernatants collected from approximately 70-80% confluent GB cells or HUVECs according to the manufacturer's instructions.

Immunoprecipitation. SNU-466, LN215-MG, U251-MG, and U373-MG cells were seeded in a 60-mm dish. After 2 days, the cells were lysed in lysis buffer (1% NP-40, 20 mM Tris-Cl, 137 mM NaCl, 2 mM EDTA, mixtures of proteinase inhibitor, and phosphatase inhibitor). Next, the lysate aliquots (1 mg/1 ml lysis buffer) were incubated with anti-NRP-1 (1:200), anti-Flt-1 (1:200), or normal IgG (1:200) antibodies, overnight at 4˚C, followed by the addition of 20 μl of Pierce Protein A Agarose (cat. no. 20333; Thermo Scientific, Inc.) for 6 h at 4˚C. Bead-bound protein was washed five times with T-TBS (2 min at 4˚C; 2,000 x g). Bound proteins were boiled with 2X Laemmli sample buffer (cat. no. 1610737; Bio-Rad Laboratories, Inc.) for 10 min and then subjected to SDS-PAGE, and assessed using western blotting.

Migration assay. Migration assays were performed using 24-Transwell plates (Corning Costar, Inc.) according to a previously described method (26). Briefly, SNU-466 and LN215-MG cells ($5x10^5$ cells/well) were seeded in six-well plates (Nunc A/S; Nalge Nunc International). After 24 h, the cells were starved under 0.2% serum containing RPMI-1640 medium for 12 h. Detached SNU-466 and LN215-MG cells ($1x10^5$ cells/1 ml 0.2% serum containing RPMI-1640 medium) were exposed with VEGF-A or Ch-ABC for 4 h. Polycarbonate filters were pre-coated with 10 mg/l fibronectin (cat. no. F0895; Sigma-Aldrich; Merck KGaA) in phosphate-buffered saline (PBS) for 1 h at room temperature. The lower chamber was filled with 500 μl of 10% fetal bovine serum containing RPMI-1640 medium. VEGF-A- or Ch-ABC-treated cells ($2x10^4$ cells/200 μl) were applied to the upper chamber for 6 h at 37˚C, and then the cells on the upper surface of the filter were removed with a cotton swab. The filters were fixed with 4% paraformaldehyde (cat. no. sc-281692; Santa Cruz Biotechnology, Inc.) for 2 h at room temperature and stained with 1% crystal violet solution (cat. no. V5265; Sigma-Aldrich; Merck KGaA) for 6 h at room temperature. The absorbance of the eluted dye using 10% (v/v) acetic acid (cat. no. 135-16; Thermo Fisher Scientific, Inc.) was measured at 560 nm using an enzyme-linked immunosorbent assay (ELISA) reader (Bio-Rad Laboratories, Inc.).

Preparation and interpretation of tissue microarray (TMA) of patients with GB. Tissue samples of patients were preserved in paraffin blocks after surgery. Pathologic diagnosis was performed with samples from 19 patients (12 males and 7 females) who had been diagnosed with GB. The samples were acquired from August 1st 2017 to July 31st 2021 at Korea University Guro Hospital (Seoul, Republic of Korea). The inclusion criteria was a sample of patients who underwent surgery, and samples of children under 18 years of age or elderly patients over 75 years of age were excluded. The mean age of the patient group was 61.4±12.3 years, and the median age was 64 years. TMA slides consisting of 57 total tissue samples from 2 to 3 different tumor sites per patient were prepared as previously described (27). After immunostaining, a pathologist provided readings on the level and presence of VEGF-A and NRP-1 through a blind review. The staining intensity was scored from none or '1+' (very weak positive) to '4+' (very strong positive). This study received ethical approval (IRB no. 2017GR330) from the Institutional Review Board of Korea University Guro Hospital (Seoul, Korea), including molecular characterization and related prognosis analysis, and written consent was obtained from patients prior to sample collection.

Xenograft tumor model. Animal care and handling procedures were performed in accordance with the Animal Research Committee Guidelines of KAIST and Korea University College of Medicine. All animal experiments were approved by the Institutional Animal Care and Use Committee of the KAIST (IACUC No. KA2013-13) and the Korea University College of Medicine (IACUC No. KOREA-2019-0123). A total of 36 female BALB/c nude mice (aged 4-5 weeks; weighing 20-25 g) were obtained from Orient Bio, Inc. All mice were raised in an animal room in a laboratory animal resource center throughout the experiments under the following

conditions: Controlled humidity, 50-60%; temperature, 25˚C; 12-h light/dark cycle and were provided with free access to food and water. The mice in all groups were intraperitoneally injected with $1x10^7$ LN215-MG cells or $3x10^7$ SNU-466 cells. The condition and behavior of the nude mice was monitored every 2 days. The mice would be humanely euthanized if they experienced unrelieved pain or distress, based on the euthanasia criteria. The groups were as follows: Group 1, PBS-treated mice (Mock, n=4); group 2, mice treated with Ch-ABC alone (n=4); group 3, mice treated with SU1498 alone (SU1498, n=4); and group 4, mice treated Ch-ABC with SU1498 (Ch-ABC/SU1498, n=6). The tumor volume and body weight were monitored throughout the study period. In all experiments, tumor dimensions were measured using calipers, and the tumor volume was calculated using the following formula: $V=0.523\ LW^2$ (L=length and W=width). When the tumors reached an average size of approximately 200 mm^3 in LN215-MG xenograft models or of approximately 100 mm^3 in SNU-466 xenograft models, the mice were intraperitoneally injected with Ch-ABC (10 mU/ml), SU1498 (10 mg/kg), or combined Ch-ABC (10 mU/ml)/SU1498 (10 mg/kg) every 3 days for 2 weeks (from day post injection, DPI 30 to DPI 42) in established mice care conditions. If the tumor volume reached 400 mm^3, sacrifice of the mice was planned, however none of the tumors of the mice in the present experiment reached that size during the experiment. The method of euthanasia used for the mice was CO_2 asphyxiation followed by cervical dislocation (CO_2 was introduced into the chamber at a rate of 30-70% of the chamber volume per min to minimize distress). After euthanizing the mice, all tumors were harvested for western blot analysis.

Statistical analysis. Data are presented as the mean ± standard deviation (SD). A two-tailed unpaired Student's t-test and Mann-Whitney test were used to determine the levels of significance for comparisons between two independent samples. Multiple group comparisons were performed using one-way analysis of variance (ANOVA) with Tukey's post hoc test, and patient survival and hazard ratio were analyzed with the log-rank (Mantel-Cox) test and the Mantel-Haenszel method. All data were analyzed using SPSS 12.0K for Windows (SPSS, Inc.) and GraphPad Prism 7 software (GraphPad Software, Inc.). P-values <0.05 were considered to indicate statistically significant differences.

Results

Expression of VEGF-A and its receptors in GB cells. In previous studies by the authors it was reported that GB cells have different sensitivities to VEGF-A signaling and that silencing VEGF-A signaling can specifically induce a significant anticancer effect in VEGF-A signaling-sensitive cells through inhibition of the autocrine signaling pathway (19,26). To further evaluate the underlying molecular mechanisms of these notable features, a sufficient number of GB cells were used. Analyzing the microarray data from the public database GEO yielded that the mRNA levels of *VEGF-A*, *Flk-1*, and *NRP-1*, but not of *Flt-1*, were significantly higher in GB tissues than in normal brain (Fig. 1A). In particular, the mRNA levels of NRP-1, VEGF-A, and Flk-1 were significantly associated with tumor grade, by contrast, the mRNA level of Flt-1 was not associated with tumor grade (Figs. 1B and S1). To verify the clinical significance between VEGF-A and NRP-1 expression, a TMA analysis of patients with GB was performed (Fig. 1C). The expression level of VEGF-A in samples from patients with GB was found to be positively associated with NRP-1 expression status (Fig. 1D, left; NRP-1 low, 0.75±0.75; NRP-1 high, 1.75±1.04; P<0.04) and vice versa (Fig. 1D, right; VEGF-A low, 2.00±0.71; VEGF-A high, 3.14±0.90; P<0.02). However, the *in vitro* expression patterns of Flt-1 and Flk-1 were variable and commonly demonstrated high expression in all nine GB cells compared to human primary astrocytes. NRP-1, which is approximately 120 kDa in molecular size, was highly expressed in SNU-489, SNU-1105, U251-MG, and U373-MG, while its expression was negative or low in A172 and SNU-626. It should be noted that in the immunoblot analysis, the NRP-1 band was uniquely shifted to a higher molecular size in SNU-466, CRT-MG, and LN215-MG cells (Fig. 1E). Significantly higher expression levels of secreted VEGF-A were also observed in the nine GB cells compared with HUVECs (Fig. 1F).

Association between sensitivity of VEGF-A signaling and the expression pattern of NRP-1 in GB cells. To validate the association between the sensitivity to autocrine VEGF-A signaling and the expression pattern of VEGF-A involving molecules, nine GB cells were incubated in the absence or presence of recombinant VEGF-A or SU1498, which is a pharmacological inhibitor against VEGF-A signaling. The viability was found to be increased by exogenous VEGF-A treatment in SNU-489, SNU-1105, U251-MG, and U373-MG cells, while the viability was not affected in A172, SNU-626, SNU-466, CRT-MG, and LN215-MG cells (Fig. 2A). A similar result was obtained using exogenous SU1498 treatment in GB cells (Fig. 2B). To achieve a more detailed investigation, two VEGF-A signaling-sensitive GB cell lines (U251-MG and U373-MG) and two VEGF-A signaling-resistant GB cell lines (SNU-466 and LN215-MG) were selected, and then the effect of transfection with si-VEGF-A or knockdown of VEGFRs on cell death was determined to elucidate the biological function of VEGF-A and its receptors in GB cells. The efficacy of knockdown of VEGF-A and VEGFRs was demonstrated by western blot analysis (Fig. 2C). The reduction in VEGF-A expression by si-VEGF-A transfection induced significant cell death in U251-MG and U373-MG cells, while the same treatment had a weak or negative cell death effect on SNU-466 and LN215-MG cells. Silencing the expression of VEGFRs by siRNA transfection also significantly induced cell death in U251-MG and U373-MG cells, but it had little effect in SNU-466 and LN215-MG cells (Fig. 2D). To further evaluate the effects of VEGF-A signaling in a different type of GB cells *in vivo*, VEGF-A signaling-sensitive U251-MG and VEGF-A signaling-resistant LN215-MG xenograft models were developed. To this end, tumor-laden mice were subcutaneously injected with control buffer or 10 mg/kg SU1498 when the tumors reached an average size of approximately 150 mm^3. U251-MG xenograft tumors treated with control buffer were found to grow to an average size of 379.19±93.36 mm^3 in 42 days after transplantation, while those treated with 10 mg/kg SU1498 grew to an average size of 200.43±46.72 mm^3 in 42 days

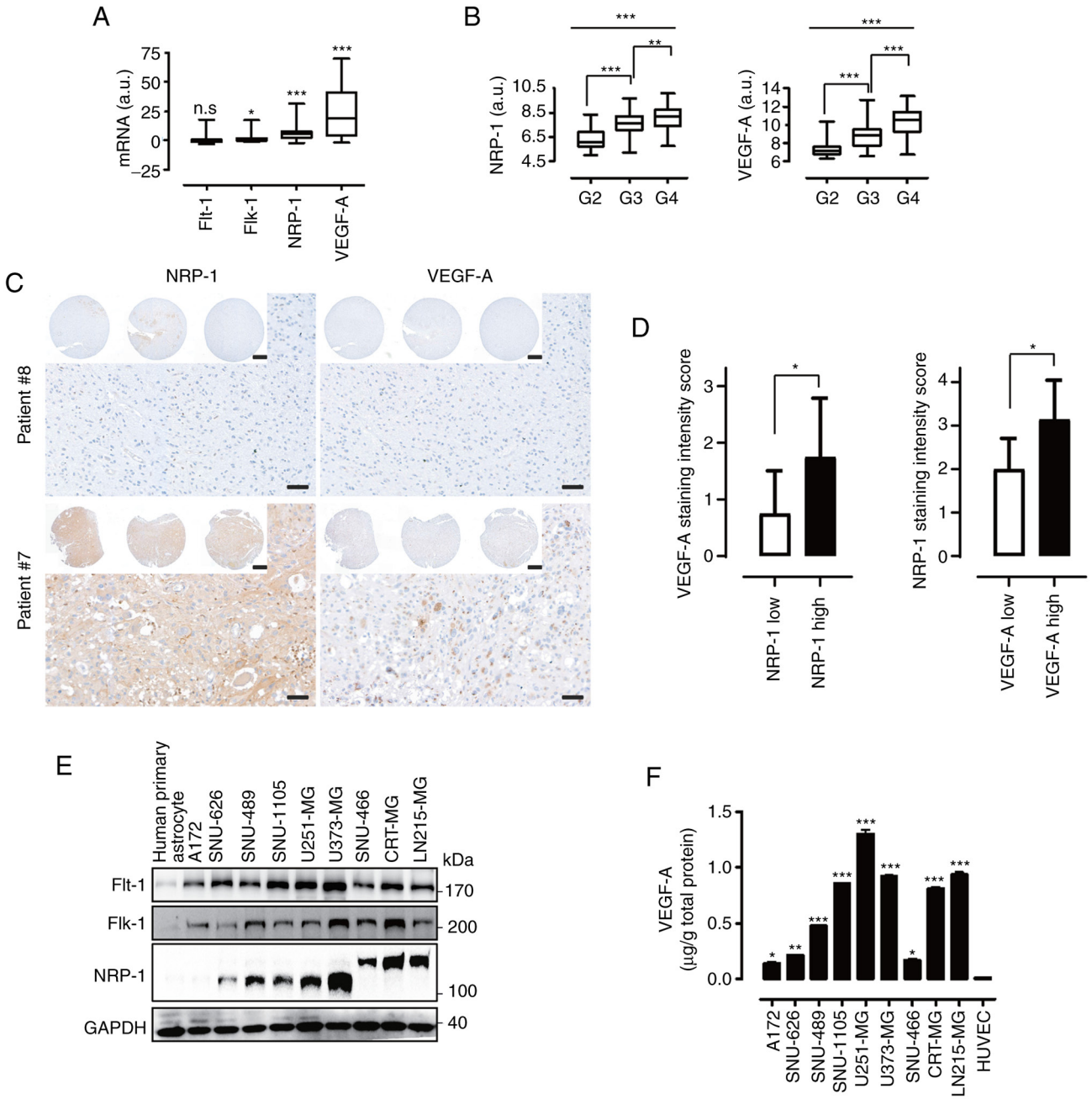

Figure 1. Expression levels of VEGF-A and its receptors in GB cells. (A) mRNA expression levels of *Flt-1*, *Flk-1*, *NRP-1*, and *VEGF-A* in brain tumors (n=144) compared with normal brain samples (n=330) analyzed using the GEO database (P-value evaluated with Student's t-test according to brain tumors vs. normal brain samples; *P<0.05 and ***P<0.001). (B) Transcriptional levels of *NRP-1* and *VEGF-A* in various grades of brain tumors analyzed using the GEO database (G indicates the tumor grade, n=3; Tukey's post hoc test was applied to significant group effects in ANOVA, P<0.0001; P-value evaluated with Student's t-test according to G2 vs. G3 and G3 vs. G4; **P<0.01 and ***P<0.001, G2; n=24, G3; n=85, G4; n=159). (C) Representative tissue microarray analysis images of patients with GB for NRP-1 and VEGF-A (scale bar, 50 μm; inlet image scale bar, 500 μm). (D) Left, comparison of VEGF-A staining intensity scores between the NRP-1 low-expression group (n=12) and high-expression group (n=8). Right, comparison of NRP-1 staining intensity scores between the VEGF-A low-expression group (n=13) and high-expression group (n=7). (E) Flt-1, Flk-1, and NRP-1 expression levels in nine GB cells and human primary astrocytes evaluated by western blot analysis. GAPDH was measured as a control. (F) ELISA was performed to quantify the expression levels of VEGF-A using the cultured supernatants from nine GB cells and HUVECs (P-value by two-tail t-tests; *P<0.05, **P<0.01 and ***P<0.001). VEGF-A, vascular endothelial growth factor-A; GB, glioblastoma; Flt-1, FMS related receptor tyrosine kinase 1; Flk-1, fetal liver kinase 1; NRP-1, neuropilin-1; GEO, Gene Expression Omnibus; GAPDH, glyceraldehyde 3-phosphate dehydrogenase; HUVECs, human umbilical vein endothelial cells; n.s, not significant.

post-transplantation (Fig. 2E). There was no significant difference in weight loss between the two groups (data not shown). By contrast, treatment with control buffer or 10 mg/kg SU1498 had no effect in LN215-MG xenograft models (Fig. 2F). No weight loss was detected in the LN215-MG xenograft models either (data not shown).

Differential intracellular signaling in VEGF-A-sensitive or VEGF-A-resistant GB cells. To elucidate the molecular mechanisms responsible for the differing sensitivity to VEGF-A signaling in GB cells, signal transduction pathways were examined following treatment with exogenous VEGF-A or SU1498. Incubation with exogenous VEGF-A

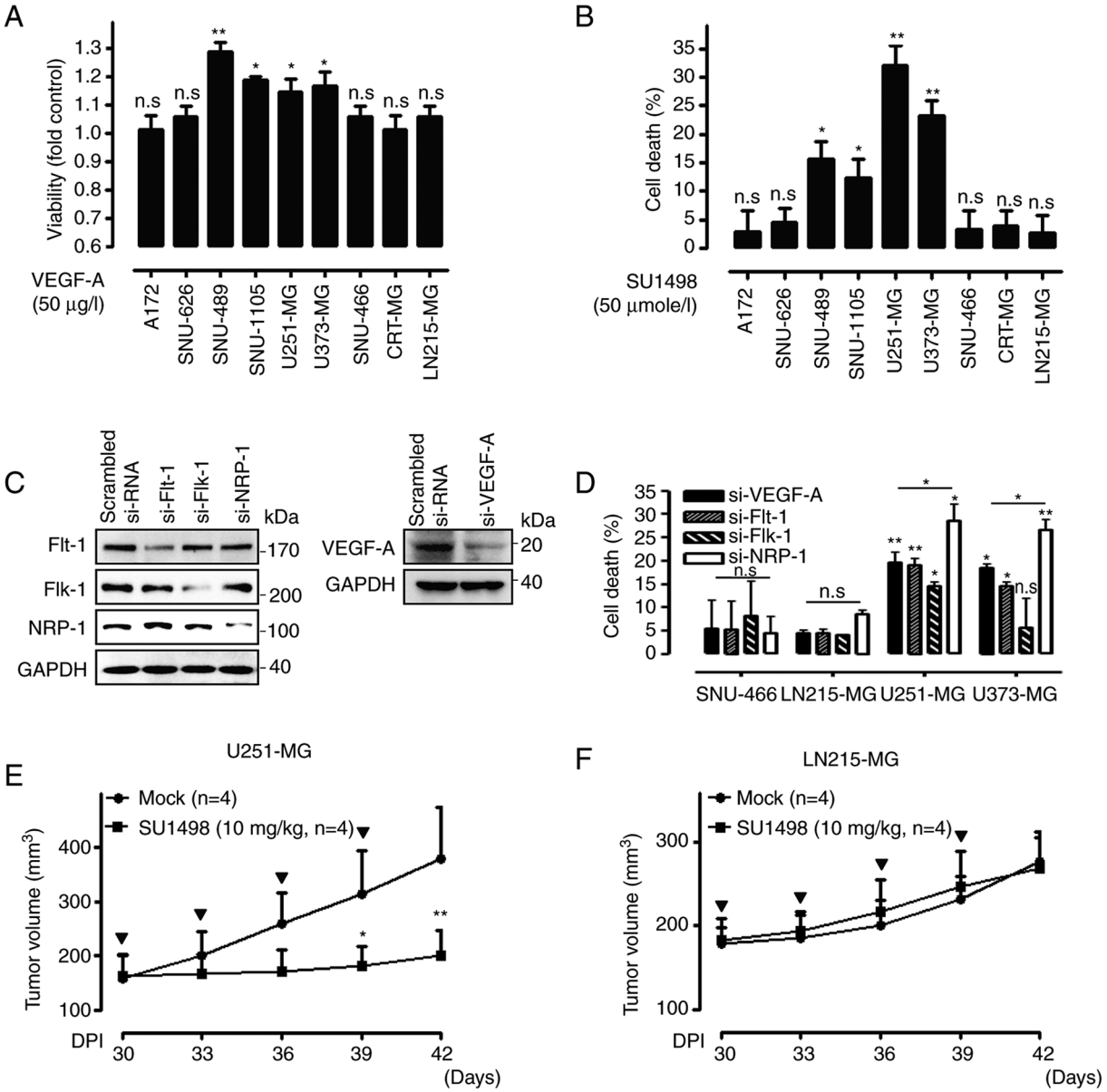

Figure 2. Effect of VEGF-A signaling in association with the expression patterns of NRP-1, on GB cells. (A and B) Nine GB cells were incubated in the absence or presence of exogenous VEGF-A (50 μg/l, left) or SU1498 (50 μmole/l, right), a VEGF receptor inhibitor, for 72 h, after which they were examined for cell viability using WST-1 assay and cell death using LDH assay (n=3; Tukey's post hoc test was applied to significant group effects in ANOVA, P<0.0001; asterisks indicate significant differences compared with the control group, *P<0.05 and **P<0.01). (C) Efficacy of Flt-1, Flk-1, NRP-1, and VEGF-A siRNA transfections assessed by western blot analysis. GAPDH was used as a control. (D) Cell death was assessed 72 h after transient transfection with siRNAs against VEGF-A, Flt-1, Flk-1, and NRP-1 using an LDH assay (n=3; Tukey's post hoc test was applied to significant group effects in ANOVA, P<0.0001; asterisks indicate significant differences compared to 0% inhibition; *P<0.05 and **P<0.01). (E) Effect of SU1498 (10 mg/kg) on the tumor volumes of U251-MG xenograft models (control group, n=4; SU1498 10 mg/kg, n=4) measured for 42 days using the following formula: V=0.523 LW^2 (L=length and W=width). Bold arrows indicate the time-points of SU1498 injection (Tukey's post-hoc test was used to determine significant group effects in ANOVA, P<0.0001; asterisks indicate significant differences between the control group and the SU1498-injected group; *P<0.05 and **P<0.01). (F) Effect of SU1498 (10 mg/kg) on the tumor volumes of LN215-MG xenograft models (control group, n=4; SU1498 10 mg/kg, n=4) measured for 42 days using the formula aforementioned, V=0.523 LW2. Bold arrows indicate the time-points of SU1498 injection. VEGF-A, vascular endothelial growth factor-A; GB, glioblastoma; NRP-1, neuropilin-1; LDH, lactate dehydrogenase; GAPDH, glyceraldehyde 3-phosphate dehydrogenase; Flt-1, FMS related receptor tyrosine kinase 1; Flk-1, fetal liver kinase 1; n.s., non-significant; si-RNA or si-, small interfering RNA.

was demonstrated to increase phosphorylation of various tyrosine residues in a time-dependent manner; in addition, treatment with SU1498 inhibited phosphorylation of tyrosine residues of various proteins compared to their basal levels in U251-MG cells (Fig. 3A). By contrast, treatment with SU1498 was not associated with any alteration of phosphotyrosine levels in LN215-MG cells (Figs. 3B and S2A). To analyze the mechanism of VEGF-A signaling in further detail, the phosphorylation levels of Flt-1, Flk-1, FAK, and AKT were examined following treatment with exogenous VEGF-A or SU1498. Treatment with VEGF-A induced the phosphorylation of Flt-1, FAK, and AKT in U251-MG cells, but not Flk-1, while SU1498 treatment produced the exact opposite effect in a time-dependent manner (Fig. 3C). By contrast, incubation with VEGF-A or SU1498 did not affect intracellular signaling in LN215-MG cells (Figs. 3D and S2B).

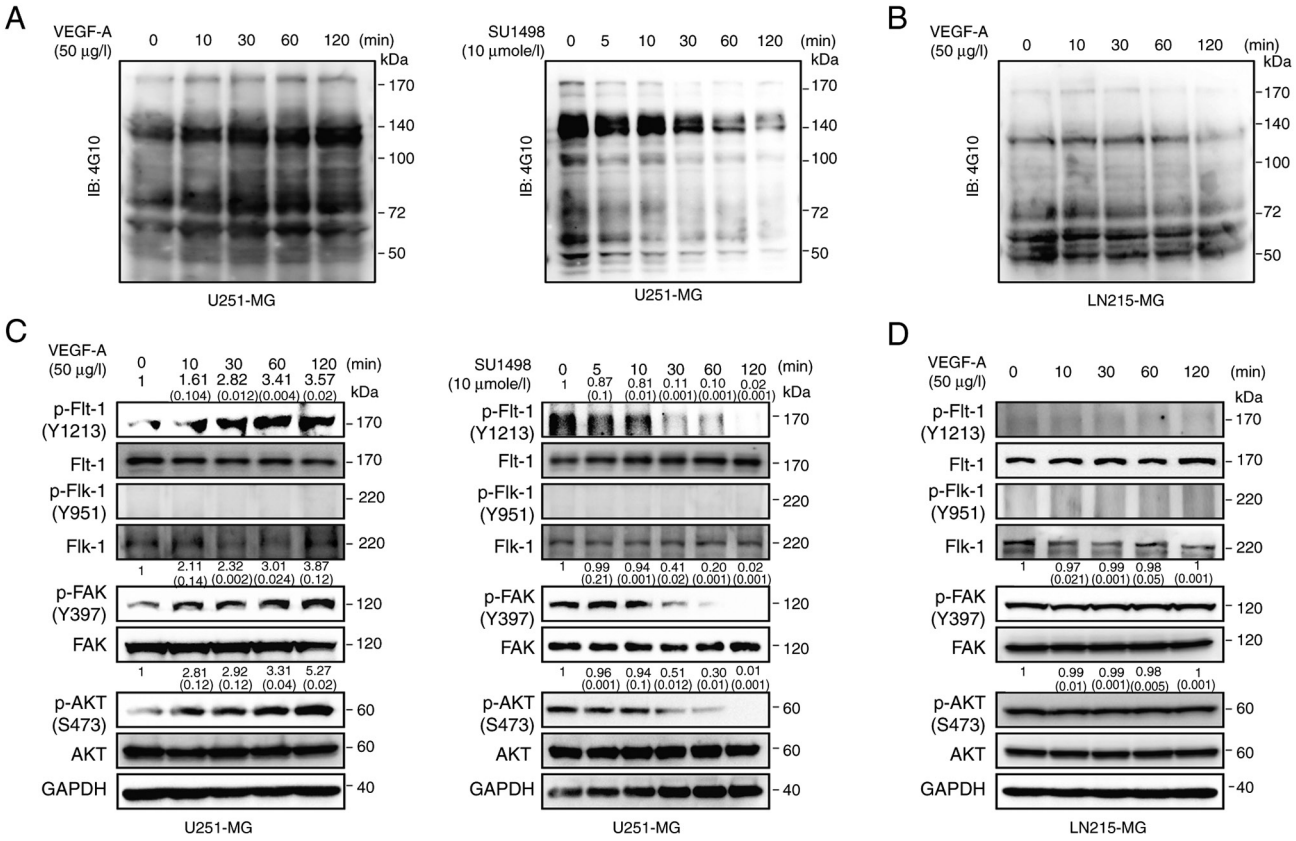

Figure 3. Intracellular signaling of VEGF-A-sensitive or VEGF-A-resistant GB cells. (A) U251-MG cells incubated with VEGF-A (50 μg/l) or SU1498 (10 μmole/l) for varying time-points, after which the cell lysates were subjected to western blot analysis using antibodies specific for total phosphotyrosine kinase, 4G10. (B) LN215-MG cells incubated with VEGF-A (50 μg/l) for varying time-points, after which the cell lysates were subjected to western blot analysis using antibodies specific for total phosphotyrosine kinase, 4G10. (C) U251-MG cells incubated with VEGF-A (50 μg/l) or SU1498 (10 μmole/l) for varying time-points, after which the cell lysates were subjected to western blot analysis using antibodies specific for p-Flt-1 (Y1213), total Flt-1, p-Flk-1 (Y951), total Flk-1, p-FAK (Y397), total FAK, p-AKT (S473), total AKT, and GAPDH. The relative pixel intensities of the target molecules were assessed by densitometric analysis using ImageJ analysis software. Data are representative of three individual experiments. (D) LN215-MG cells incubated with VEGF-A (50 μg/l) for varying time-points, after which the cell lysates were subjected to western blot analysis using antibodies specific for p-Flt-1 (Y1213), total Flt-1, p-Flk-1 (Y951), total Flk-1, p-FAK (Y397), total FAK, p-AKT (S473), total AKT, and GAPDH. The relative pixel intensities of the target molecules were assessed by densitometric analysis using ImageJ analysis software. Data are representative of three individual experiments. VEGF-A, vascular endothelial growth factor-A; GB, glioblastoma; p-, phosphorylated; Flt-1, FMS related receptor tyrosine kinase 1; Flk-1, fetal liver kinase 1; GAPDH, glyceraldehyde 3-phosphate dehydrogenase.

Physical interaction between wild-type NRP-1 and Flt-1 in VEGF-A signaling-sensitive GB cells. Since research has reported that the function of NRP-1 is associated with Flt-1 and Flk-1 (8,9), the molecular interaction between VEGFRs and NRP-1 was next examined using immunoprecipitation. In VEGF-A signaling-sensitive U251-MG and U373-MG cells, NRP-1 exclusively interacted with functional Flt-1, whereas no molecular interaction was observed in VEGF-A signaling-resistant LN215-MG and SNU-466 cells (Fig. 4A and B). The interaction between NRP-1 and Flt-1 was intensified by exogenous VEGF-A treatment (Fig. 4C), whereas the reduction in NRP-1 expression by si-NRP-1 transfection weakened its interaction with Flt-1 (Fig. 4D).

Restoring VEGF-A signaling after eliminating chondroitin sulfate modification of NRP-1 in VEGF-A signaling-resistant GB cells. It was next demonstrated whether NRP-1 could be modified by chondroitin sulfate using Ch-ABC, which is an enzyme that cleaves GAG from membrane surface proteoglycans in LN215-MG cells. Treatment with Ch-ABC effectively removed the higher molecular weight band with a concomitant increase of 120 kDa NRP-1. The phosphorylation levels of FAK and AKT were also increased by Ch-ABC treatment in LN215-MG cells (Fig. 5A). Furthermore, an interaction between NRP-1 and Flt-1 was observed after eliminating chondroitin sulfate modification of NRP-1 in LN215-MG cells, and Flt-1 which interacted with NRP-1 was found to be phosphorylated (Fig. 5B). To investigate the molecular function of chondroitin sulfate modification of NRP-1 in VEGF-A signaling-resistant GB cells, SNU-466 and LN215-MG cells were incubated in the absence or presence of Ch-ABC, and then malignant features were assessed. Proliferation and migration stimulated by VEGF-A signaling were recovered by combined treatment with Ch-ABC in SNU-466 and LN215-MG cells (Fig. 5C). The significance of combination treatment with VEGF-A and Ch-ABC was validated by immunoblot analysis. Combined treatment with VEGF-A and Ch-ABC increased the phosphorylation of FAK and AKT relative to that of VEGF-A treatment in LN215-MG cells (Fig. 5D). In adition, eliminating the chondroitin sulfate modification with Ch-ABC significantly increased the cytotoxicity of SU1498 in SNU-466 and LN215-MG cells in a dose-dependent manner (Fig. 5E).

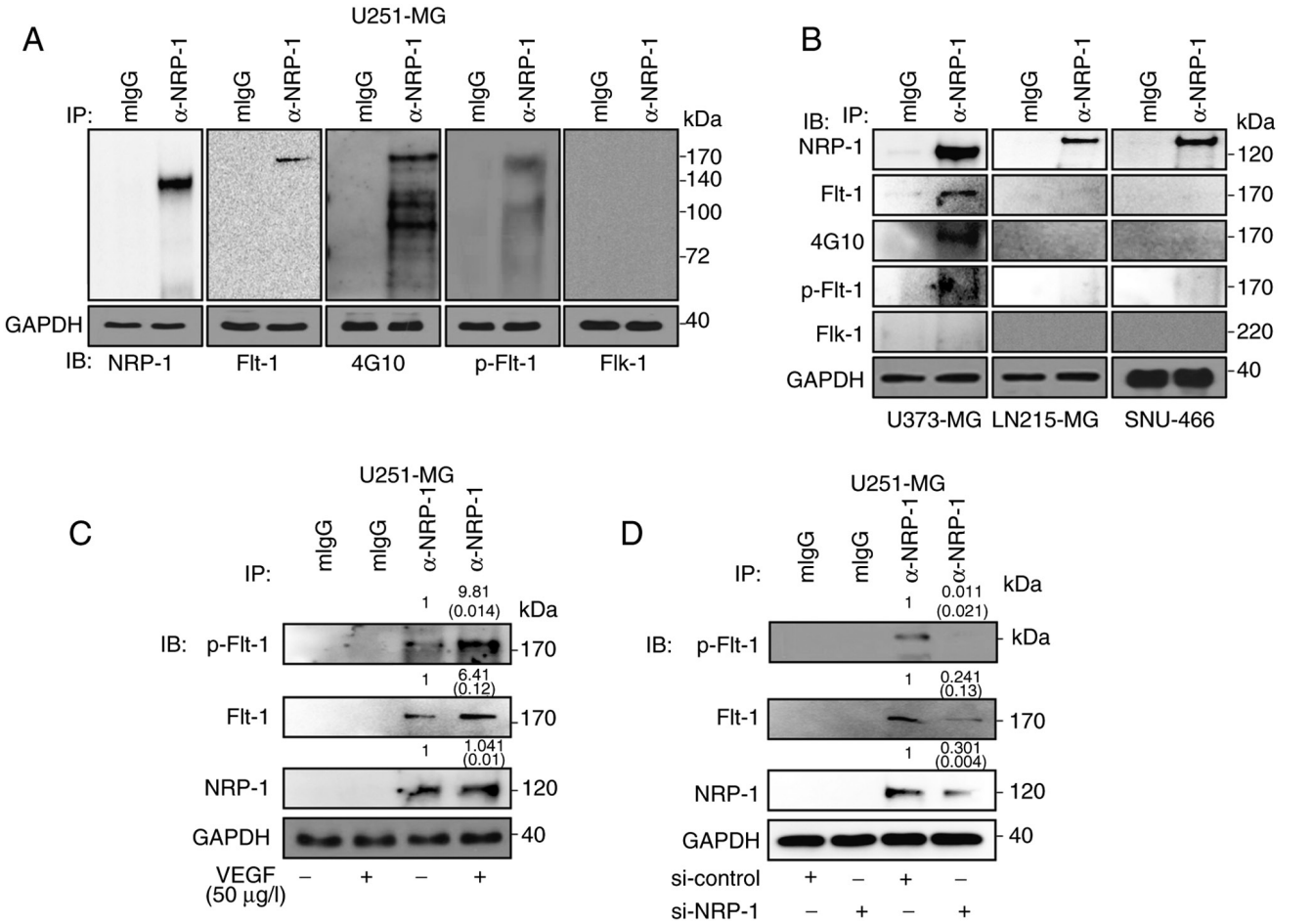

Figure 4. Physical interaction of wild-type NRP-1 and Flt-1 in VEGF-A-sensitive GB cells. (A) Interaction between NRP-1 and Flt-1 or Flk-1 analyzed by immunoprecipitation using 1% NP-40 lysis buffer in U251-MG cells. (B) Interaction between NRP-1 and Flt-1 or Flk-1 analyzed by immunoprecipitation using 1% NP-40 lysis buffer in U373-MG, CRT-MG, and LN215-MG cells. GAPDH was used as a control. (C) An increase in interaction between NRP-1 and Flt-1 was determined using western blot analysis following exogenous VEGF-A treatment. The relative pixel intensities of the target molecules were assessed by densitometric analysis using ImageJ analysis software. Data are representative of three individual experiments. (D) A decrease in interaction between NRP-1 and Flt-1 analyzed by western blot analysis following NRP-1 siRNA transfection. The relative pixel intensities of the target molecules were assessed by densitometric analysis using ImageJ analysis software. Data are representative of three individual experiments. NRP-1, neuropilin-1; Flt-1, FMS related receptor tyrosine kinase 1; VEGF-A, vascular endothelial growth factor-A; GB, glioblastoma; Flk-1, fetal liver kinase 1; GAPDH, glyceraldehyde 3-phosphate dehydrogenase; siRNA or si-, small interfering RNA.

The significant effect of combination treatment with SU1498 and Ch-ABC was also confirmed by immunoblot analysis (Fig. 5F).

In vivo effect of eliminating chondroitin sulfate modification in VEGF-A signaling-resistant GB cells. To further validate the restoration of VEGF-A signaling by eliminating chondroitin sulfate modification in VEGF-A-resistant GB cells *in vivo*, LN215-MG and SNU-466 xenograft models were developed. When their tumors reached an average size of approximately 200 mm^3, tumor-laden mice were subcutaneously injected with either control buffer, 10 mU/ml Ch-ABC, 10 mg/kg SU1498, or a combination of SU1498 and Ch-ABC. At 42 days after transplantation, LN215-MG xenograft tumors treated with control buffer had grown to an average size of 290.74±12.53 mm^3 whereas those treated with both 10 mU/ml Ch-ABC and 10 mg/kg SU1498 had grown to an average size of 227.43±16.65 mm^3. Administration of 10 mU/ml Ch-ABC or 10 mg/kg SU1498 had no effect in LN215-MG xenograft models (Fig. 6A). In addition, there were no differences in weight loss between groups (data not shown). SNU-466 xenograft tumors treated with control buffer grew to an average size of 234.33±13.77 mm^3 in 42 days after transplantation while those treated with a combination of 10 mU/ml Ch-ABC and 10 mg/kg SU1498 grew to an average size of 193.67±14.67 mm^3 in the same time-frame. Treatment with 10 mU/ml Ch-ABC or 10 mg/kg SU1498 had no effect in SNU-466 xenograft models (Fig. 6B). There was no significant difference in weight loss either (data not shown). To ascertain the *in vivo* anti-growth effect, caspase-3-mediated apoptosis in the LN215-MG xenograft model was investigated. Concurrent treatment with 10 mU/ml Ch-ABC and 10 mg/kg SU1498 was shown to induce cleavage of caspase-3 in VEGF-A-resistant the LN215-MG xenograft model (Fig. 6C). Based on the *in vivo* findings indicating that chondroitin sulfate modifications may affect GB cell malignancies, a TMA analysis of patients with GB was conducted to determine whether the level of

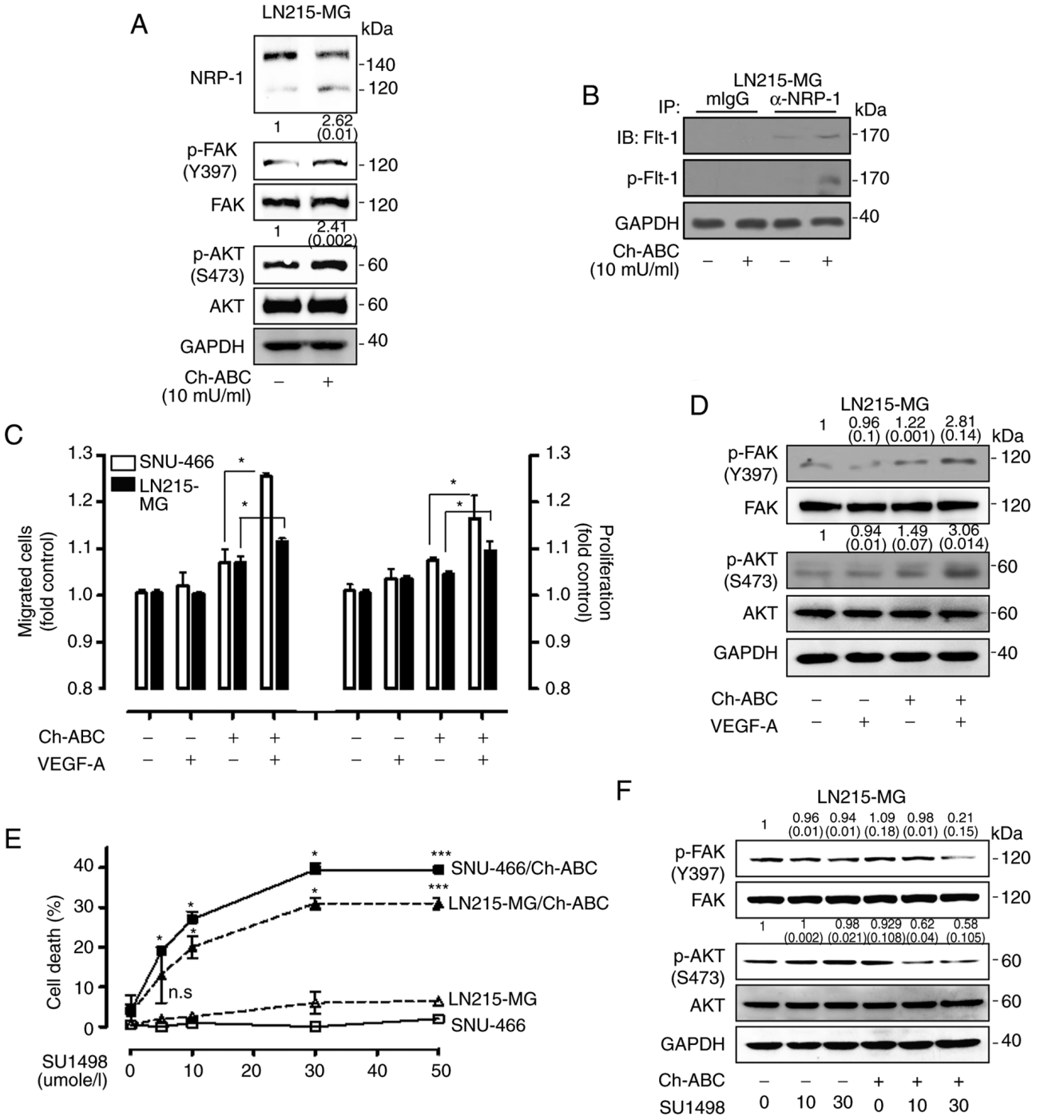

Figure 5. Effect of eliminating chondroitin sulfate modification on NRP-1 in GB cells. (A) Elimination of chondroitin sulfate modification on NRP-1 using Ch-ABC (10 mU/ml) treatment in LN215-MG cells, after which the cell lysates were subjected to western blot analysis using antibodies specific for NRP-1, p-FAK (Y397), total FAK, p-AKT (S473), and total AKT. GAPDH was used as a control. The relative pixel intensities of the target molecules were assessed by densitometric analysis using ImageJ analysis software. Data are representative of three individual experiments. (B) An increase in interaction between NRP-1 and Flt-1 was determined by immunoprecipitation using 1% NP-40 lysis buffer in LN215-MG cells following Ch-ABC treatment. The relative pixel intensities of the target molecules were assessed by densitometric analysis using ImageJ analysis software. GAPDH was used as a control. Data are representative of three individual experiments. (C) SNU-466 and LN215-MG cells incubated with or without Ch-ABC in the absence or presence of VEGF-A (50 μg/l) for 4 h (migration) or 72 h (proliferation). VEGF-mediated cell migration was assessed using Transwell migration assay (left) and proliferation was evaluated by WST-1 assay (right) (P-values were evaluated with Student's t-tests). (D) LN215-MG pretreated with or without Ch-ABC for 24 h in the absence or presence of VEGF-A (50 μg/l) for 120 min, after which the LN215-MG cell lysates were subjected to western blot analysis using antibodies specific for p-FAK (Y397), total FAK, p-AKT (S473), and total AKT. GAPDH was used as a control. The relative pixel intensities of the target molecules were assessed by densitometric analysis using ImageJ analysis software. Data are representative of three individual experiments. (E) SNU-466 and LN215-MG cells were incubated with SU1498 in a dose-dependent manner in the absence or presence of Ch-ABC for 24 h. Cell death was assessed using an LDH assay (n=3; Tukey's post hoc test was applied to significant group effects in ANOVA; *P<0.05 and ***P<0.005). (F) LN215-MG cells were incubated with SU1498 in a dose-dependent manner in the absence or presence of Ch-ABC for 24 h, after which the cell lysates were subjected to western blot analysis using antibodies specific for p-FAK (Y397), total FAK, p-AKT (S473), and total AKT. GAPDH was used as a control. The relative pixel intensities of the target molecules were assessed by densitometric analysis using ImageJ analysis software. Data are representative of three individual experiments. NRP-1, neuropilin-1; GB, glioblastoma; Ch-ABC, chondrotinase ABC; p-, phosphorylated; Flt-1, FMS related receptor tyrosine kinase 1; GAPDH, glyceraldehyde 3-phosphate dehydrogenase; VEGF-A, vascular endothelial growth factor-A.

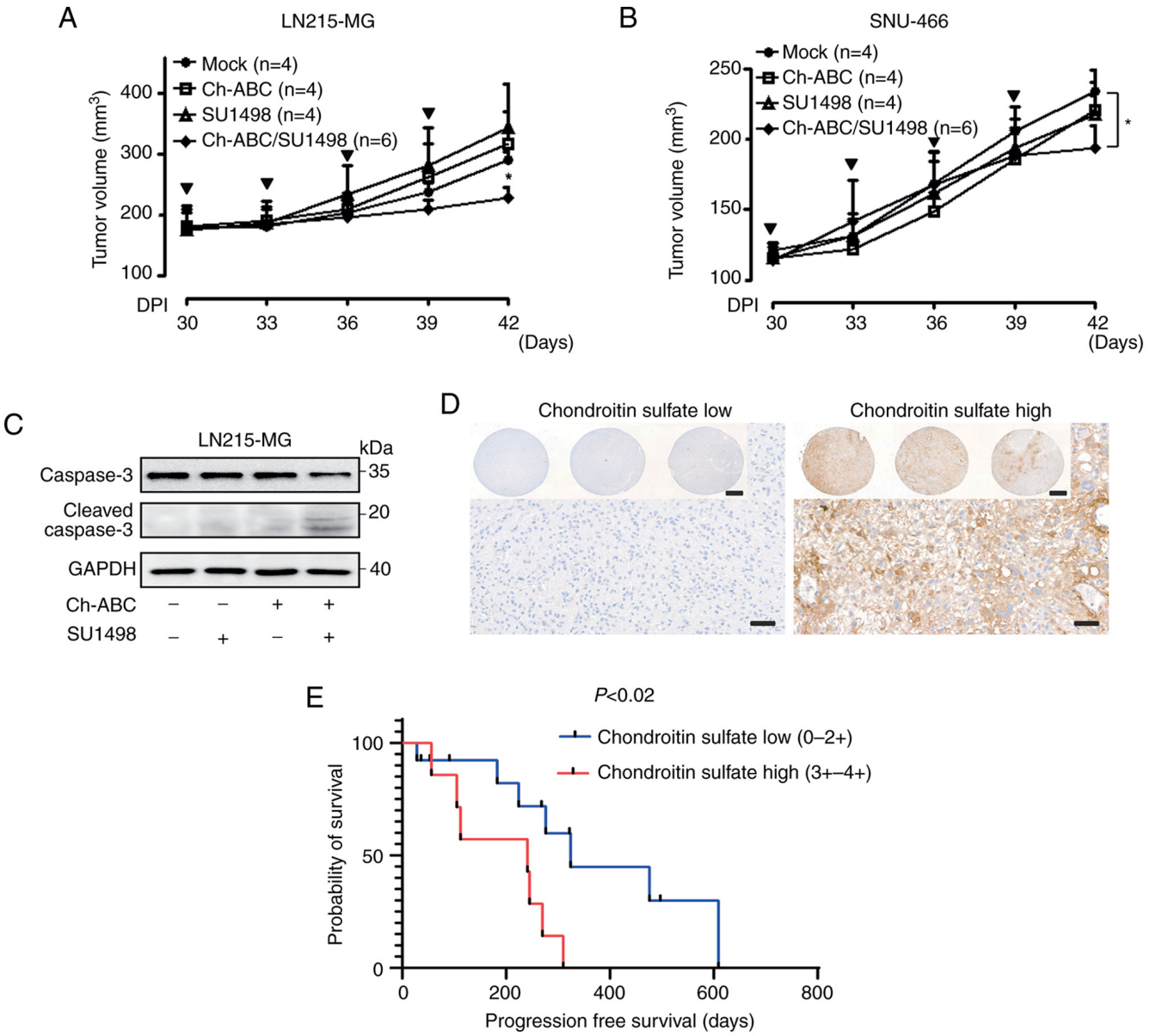

Figure 6. Resensitization of VEGF-A signaling through the elimination of chondroitin sulfate modification in GB cells. (A) Effect of Ch-ABC (10 mU/ml), SU1498 (10 mg/kg), or Ch-ABC/SU1498 (10 mU/ml/10 mg/kg) on the tumor volumes of LN215-MG xenograft models (control group, n=4; Ch-ABC, n=4; SU1498, n=4; and Ch-ABC/SU1498, n=6) measured for 42 days using the following formula: V=0.523 LW2 (L=length and W=width). Bold arrows indicate the time-points of Ch-ABC, SU1498, or Ch-ABC/SU1498 injection (Tukey's post-hoc test was used to determine significant group effects in ANOVA, P<0.0001; asterisks indicate significant differences between the control group and the Ch-ABC, SU1498, or Ch-ABC/SU1498 group; *P<0.05). (B) Effect of Ch-ABC (10 mU/ml), SU1498 (10 mg/kg), or Ch-ABC/SU1498 (10 mU/ml/10 mg/kg) on the tumor volumes of SNU-466 xenograft models (control group, n=4; Ch-ABC, n=4; SU1498, n=4; and Ch-ABC/SU1498, n=6) measured for 42 days using the aforementioned formula: V=0.523 LW^2. Bold arrows indicate the time-points of Ch-ABC, SU1498, or Ch-ABC/SU1498 injection (Tukey's post-hoc test was used to determine significant group effects in ANOVA, P<0.0001; asterisks indicate significant differences between the control group and the Ch-ABC, SU1498, or Ch-ABC/SU1498 group; *P<0.05). (C) Lysates derived from LN215-MG xenograft tumor samples were assessed for caspase-3, cleaved caspase-3, and GAPDH using western blot analysis. Data are representative of three individual experiments. (D) Representative tissue microarray analysis images of chondroitin sulfate expression of patients with GB (scale bar, 50 μm; inlet image scale bar, 500 μm). (E) Association between chondroitin sulfate expression and progression-free survival of GB patients. The survival analysis of 19 patients with GB was performed by integrating the clinical data of patients with GB with their chondroitin sulfate expression levels. VEGF-A, vascular endothelial growth factor-A; GB, glioblastoma; Ch-ABC, chondrotinase ABC.

chondroitin sulfate expression could affect the prognosis of patients GB (Fig. 6D). As revealed in Fig. 6E, the group with high expression of chondroitin sulfate exhibited poor progression-free survival compared with the group with low expression (P<0.02; hazard ratio, 4.938; 95% confidence interval, 1.34-18.16), although there was no statistical difference in overall survival (Fig. S3).

Discussion

In the present study, the associations between the expression types of NRP-1 and the susceptibility of GB cells to VEGF-A signaling were revealed both *in vitro* and *in vivo*. Differential dependency to VEGF-A signaling was classified according to the interaction between NRP-1 and Flt-1. It was further

confirmed that re-sensitization of VEGF-A signaling could be achieved by eliminating the chondroitin sulfate modification of NRP-1 in VEGF-A signaling-resistant GB cells both *in vitro* and *in vivo*. Chondroitin sulfate modification was also found to be associated with an adverse prognosis in patients with GB. To the best of our knowledge, this is the first study to report that anti-VEGF-A therapies that involve the elimination of chondroitin sulfate modification of NRP-1, may represent innovative therapeutic approaches for patients with GB who exhibit no response to treatments targeting the VEGF-A signaling pathway.

Due to the increasing number of failed clinical trials attempting to use angiogenesis inhibitors for cancer therapies, there has been growing interest in the mechanisms underlying autocrine VEGF-A signaling (28). Research has shown that some patients with GB temporarily benefit from a single VEGF-A targeting therapy or combination therapies with antitumor drugs (2). However, the majority of patients with GB are entirely refractory to anti-VEGF-A therapies. The cause of this may be attributable to the acquisition of resistance to anti-VEGF-A therapies due to alternative signaling pathways (29-32). In the present study, potential VEGF-A therapies exploiting the autocrine VEGF-A signaling involved in NRP-1 expression types were revealed. It was demonstrated that silencing of VEGF-A signaling by siRNA transfection or pharmacological inhibitor treatment resulted in two types of outcomes *in vitro* and *in vivo* based on the expression pattern of NRP-1. Furthermore, the differential sensitivity was accompanied by a convincing intracellular signaling pathway difference, indicating that prudent grouping of patients with GB to target VEGF-A signaling should be performed based on the expression types of NRP-1.

VEGF-A and its receptors were originally investigated in endothelial cells in angiogenesis (33). Flk-1 (also known as VEGF-R2), has been defined as a critical signaling receptor for VEGF-A-mediated mitogenesis, vascular permeability, and angiogenesis due to its strong tyrosine kinase activity. By comparison, Flt-1 (also known as VEGF-R1), has weak tyrosine kinase activity, which leads Flt-1 to be a supplemented receptor for Flk-1 in angiogenesis (34). However, several research groups have suggested that the mediation of Flt-1 by VEGF-A signaling affects survival in lymphoma, leukemia, prostate cancer, colon cancer, and neuroblastoma (35-39). VEGF-A signaling has also been reported to involve a combined function of Flt-1 and Flk-1 on survival in primary glioblastoma cells (40). At present, Flt-1 is the specific receptor associated with autocrine VEGF-A signaling based on its capability to interact with wild-type NRP-1 in GB cells.

NRP-1 has been reported to have a functional role in tumorigenesis and prognosis in various malignant tumors (38,41-44). Furthermore, research has shown that enhanced NRP-1 expression promotes glioma progression *in vivo* through a HGF/SF and HGFR signaling-independent VEGF-A signaling pathway (10). In addition, NRP-1 has also been suggested to have a tumorigenesis-suppressive function in pancreatic cells (43) and was demonstrated to have improved prognosis in colon cancers (45). The results of the present study reveal that chondroitin sulfate-modified NRP-1 could numb the sensitivity to VEGF-A signaling, while the removal of this chondroitin sulfate modification on NRP-1 led to re-sensitization to VEGF-A signaling by restoring the interaction with Flt-1, thus indicating that the existence or non-existence of chondroitin-sulfated modification on NRP-1 may be a critical factor for determining the effectiveness of therapies targeting VEGF-A signaling. To determine the association between the expression pattern of NRP-1 and sensitivity to VEGF-A signaling more clearly, it should be considered whether the smeary minor bands of the western blotting results are a natural property of GB cells or a minor experimental discrepancy. It has recently been reported that targeting endogenous VEGF-A or NRP-1 does not directly decrease tumor cell growth or invasion, and that the anticancer effect is instead due to an anti-angiogenic effect in endothelial cells (44,46,47). However, no studies have examined the role of NRP-1 depending on the status of its expression pattern. It was also observed that the co-administration of Ch-ABC and SU1498 had a relatively moderate *in vivo* anticancer effect, contrary to the *in vitro* results. The limited effect of targeting VEGF-A signaling with the elimination of chondroitin sulfate modification of NRP-1 may be attributable to the non-specific elimination by Ch-ABC in LN215-MG and SNU-466 xenograft models. Thus, to improve this innovative therapy, a direct reagent or technique for eliminating chondroitin sulfate modification on NRP-1 should be developed, i.e., 'the pincer attack'. In addition, derestricted GAGs have been reported to be correlated with clinical outcomes in various malignant tumors (18). Consistent with the results of this previous study, it was revealed that chondroitin sulfate modification was associated with adverse prognosis in patients with GB. To further elucidate the association between chondroitin sulfate modification on NRP-1 and clinical outcomes in patients with GB, future studies should be performed using a large number of tissue samples from patients with GB. Based on our preliminary results associated with detecting the expression type of NRP-1 in whole blood samples of patients with GB, application of the technique to determine the association between chondroitin-sulfated NRP-1 and wild-type NRP-1 expression in whole blood samples from patients with GB could not be ignored.

Recent studies have suggested that soluble NRP-1 can be detected both *in vitro* and *in vivo* through the functional role of a metalloprotease such as ADAM10 (48-50). In agreement with these previous studies, preliminary results indicating that chondroitin sulfate-modified soluble NRP-1 can be detected in GB cells were obtained using accessible techniques such as ELISA and immunoprecipitation (Fig. S4). These encouraging results suggest that the detection of wild-type NRP-1 and modified NRP-1 could potentially be achieved using human materials such as whole blood, saliva, and urine, which would lead to widespread practical applications. The use of this classifying technique of NRP-1 expression pattern from human materials may be an innovative therapeutic approach achieved using various inhibitors against VEGF-A signaling for patients with GB.

In summary, the results of the present study provide a basis that may be of aid in variable or disappointing outcomes among patients with GB to therapies targeting VEGF-A signaling in clinical trials. The present study also offers a rationale for further research to develop innovative strategies targeting VEGF-A signaling by eliminating the modification from NRP-1.

Acknowledgements

We would like to thank Professor Etty N. Benveniste (University of Alabama, Birmingham, USA) for providing the U251-MG, U373-MG, CRT-MG, and LN215-MG cells and Professor In-Hong Choi (Yonsei University, Seoul, Korea) for providing the human normal astrocytes.

Funding

The present research was supported by the Bio & Medical Technology Development Program of the National Research Foundation (NRF) of Korea funded by the Ministry of Science and ICT (grant no. 2016M3A9B6945831) and (grant no. 2017M3A9G8084516). The research was also supported by the NRF of the Republic of Korea (grant no. 2016R1A6A1A03012862) and (grant no. NRF-2019M3A9E2061791).

Availability of data and materials

The data generated in the present study are included in the figures and supplementary figures of this article.

Authors' contributions

JWL and CC conceived and designed the study. JWL, KChong, and JSL developed the methodology. JWL, KChong, JSL, and CK contributed to the acquisition of the data, animals, and facilities as well as the management of the data of patients. JWL, KChong, JSL, JHK, CK, KChoi, and CC analyzed and interpreted the data (e.g., statistical analysis, biostatistics, computational analysis). JWLee, KChong, and CC wrote, reviewed, and/or revised the manuscript. JWL and CC supervised the study. JWL and KChong confirm the authenticity of all the raw data. All authors read and approved the manuscript and agree to be accountable for all aspects of the research in ensuring that the accuracy or integrity of any part of the work are appropriately investigated and resolved.

Ethics approval and consent to participate

The patient sample study complied with the guidelines and protocols approved by the Institutional Review Board (IRB no. 2017GR330) of Korea University Guro Hospital (Seoul, Korea). Written informed consent was obtained prior to sample collection from all the participants who agreed to the use of their samples in scientific research, and procedures were conducted according to the Declaration of Helsinki. Animal care and handling procedures were performed in accordance with Animal Research Committee's Guidelines of KAIST and Korea University College of Medicine. All animal experiments were approved by the Institutional Animal Care and Use Committee of the KAIST (IACUC No. KA2013-13) and the Korea University College of Medicine (IACUC No. KOREA-2019-0123).

Patient consent for publication

Not applicable.

Competing interests

CC is the founder and shareholder, and KChoi is a minor shareholder of ILIAS Biologics, Inc. The other authors declare that they have no competing interests.

References

1. Siegel RL, Miller KD and Jemal A: Cancer statistics, 2018. CA Cancer J Clin 68: 7-30, 2018.
2. Stupp R, Mason WP, van den Bent MJ, Weller M, Fisher B, Taphoorn MJ, Belanger K, Brandes AA, Marosi C, Bogdahn U, *et al*: Radiotherapy plus concomitant and adjuvant temozolomide for glioblastoma. N Engl J Med 352: 987-996, 2005.
3. Westphal M and Lamszus K: The neurobiology of gliomas: From cell biology to the development of therapeutic approaches. Nat Rev Neurosci 12: 495-508, 2011.
4. Louis DN, Ohgaki H, Wiestler OD, Cavenee WK, Burger PC, Jouvet A, Scheithauer BW and Kleihues P: The 2007 WHO classification of tumours of the central nervous system. Acta Neuropathol 114: 97-109, 2007.
5. Ohgaki H and Kleihues P: Population-based studies on incidence, survival rates, and genetic alterations in astrocytic and oligodendroglial gliomas. J Neuropathol Exp Neurol 64: 479-489, 2005.
6. Miller CR and Perry A: Glioblastoma. Arch Pathol Lab Med 131: 397-406, 2007.
7. Newton HB: Primary brain tumors: Review of etiology, diagnosis and treatment. Am Fam Physician 49: 787-797, 1994.
8. Soker S, Takashima S, Miao HQ, Neufeld G and Klagsbrun M: Neuropilin-1 is expressed by endothelial and tumor cells as an isoform-specific receptor for vascular endothelial growth factor. Cell 92: 735-745, 1998.
9. Gu C, Rodriguez ER, Reimert DV, Shu T, Fritzsch B, Richards LJ, Kolodkin AL and Ginty DD: Neuropilin-1 conveys semaphorin and VEGF signaling during neural and cardiovascular development. Dev Cell 5: 45-57, 2003.
10. Hu B, Guo P, Bar-Joseph I, Imanishi Y, Jarzynka MJ, Bogler O, Mikkelsen T, Hirose T, Nishikawa R and Cheng SY: Neuropilin-1 promotes human glioma progression through potentiating the activity of the HGF/SF autocrine pathway. Oncogene 26: 5577-5586, 2007.
11. Ellis LM: The role of neuropilins in cancer. Mol Cancer Ther 5: 1099-1107, 2006.
12. Evans IM, Yamaji M, Britton G, Pellet-Many C, Lockie C, Zachary IC and Frankel P: Neuropilin-1 signaling through p130Cas tyrosine phosphorylation is essential for growth factor-dependent migration of glioma and endothelial cells. Mol Cell Biol 31: 1174-1185, 2011.
13. Frankel P, Pellet-Many C, Lehtolainen P, D'Abaco GM, Tickner ML, Cheng L and Zachary IC: Chondroitin sulphate-modified neuropilin 1 is expressed in human tumour cells and modulates 3D invasion in the U87MG human glioblastoma cell line through a p130Cas-mediated pathway. EMBO Rep 9: 983-989, 2008.
14. Miao HQ, Lee P, Lin H, Soker S and Klagsbrun M: Neuropilin-1 expression by tumor cells promotes tumor angiogenesis and progression. FASEB J 14: 2532-2539, 2000.
15. Parikh AA, Fan F, Liu WB, Ahmad SA, Stoeltzing O, Reinmuth N, Bielenberg D, Bucana CD, Klagsbrun M and Ellis LM: Neuropilin-1 in human colon cancer: Expression, regulation, and role in induction of angiogenesis. Am J Pathol 164: 2139-2151, 2004.
16. Shintani Y, Takashima S, Asano Y, Kato H, Liao Y, Yamazaki S, Tsukamoto O, Seguchi O, Yamamoto H, Fukushima T, *et al*: Glycosaminoglycan modification of neuropilin-1 modulates VEGFR2 signaling. EMBO J 25: 3045-3055, 2006.
17. Kjellen L and Lindahl U: Proteoglycans: Structures and interactions. Annu Rev Biochem 60: 443-475, 1991.
18. Theocharis AD, Tsolakis I, Tzanakakis GN and Karamanos NK: Chondroitin sulfate as a key molecule in the development of atherosclerosis and cancer progression. Adv Pharmacol 53: 281-295, 2006.
19. Lee J, Ku T, Yu H, Chong K, Ryu SW, Choi K and Choi C: Blockade of VEGF-A suppresses tumor growth via inhibition of autocrine signaling through FAK and AKT. Cancer Lett 318: 221-225, 2012.

20. Piccolo SR, Withers MR, Francis OE, Bild AH and Johnson WE: Multiplatform single-sample estimates of transcriptional activation. Proc Natl Acad Sci USA 110: 17778-17783, 2013.
21. Irizarry RA, Hobbs B, Collin F, Beazer-Barclay YD, Antonellis KJ, Scherf U and Speed TP: Exploration, normalization, and summaries of high density oligonucleotide array probe level data. Biostatistics 4: 249-264, 2003.
22. Dai M, Wang P, Boyd AD, Kostov G, Athey B, Jones EG, Bunney WE, Myers RM, Speed TP, Akil H, *et al*: Evolving gene/transcript definitions significantly alter the interpretation of GeneChip data. Nucleic Acids Res 33: e175, 2005.
23. Lee J, Lee J, Yun JH, Choi C, Cho S, Kim SJ and Kim JH: Autocrine DUSP28 signaling mediates pancreatic cancer malignancy via regulation of PDGF-A. Scientific reports 7: 12760, 2017.
24. Lee J, Lee J, Sim W and Kim JH: Soluble TGFBI aggravates the malignancy of cholangiocarcinoma through activation of the ITGB1 dependent PPARγ signalling pathway. Cell Oncol (Dordr) 45: 275-291, 2022.
25. Lee J, Kim DH and Kim JH: Combined administration of naringenin and hesperetin with optimal ratio maximizes the anti-cancer effect in human pancreatic cancer via down regulation of FAK and p38 signaling pathway. Phytomedicine 58: 152762, 2019.
26. Lee J, Lee J, Yun JH, Choi C, Cho S, Kim SJ and Kim JH: Autocrine DUSP28 signaling mediates pancreatic cancer malignancy via regulation of PDGF-A. Sci Rep 7: 12760, 2017.
27. Reddy SP, Britto R, Vinnakota K, Aparna H, Sreepathi HK, Thota B, Kumari A, Shilpa BM, Vrinda M, Umesh S, *et al*: Novel glioblastoma markers with diagnostic and prognostic value identified through transcriptome analysis. Clin Cancer Res 14: 2978-2987, 2008.
28. Vasudev NS and Reynolds AR: Anti-angiogenic therapy for cancer: Current progress, unresolved questions and future directions. Angiogenesis 17: 471-494, 2014.
29. Batchelor TT, Sorensen AG, di Tomaso E, Zhang WT, Duda DG, Cohen KS, Kozak KR, Cahill DP, Chen PJ, Zhu M, *et al*: AZD2171, a pan-VEGF receptor tyrosine kinase inhibitor, normalizes tumor vasculature and alleviates edema in glioblastoma patients. Cancer Cell 11: 83-95, 2007.
30. Sabir A, Schor-Bardach R, Wilcox CJ, Rahmanuddin S, Atkins MB, Kruskal JB, Signoretti S, Raptopoulos VD and Goldberg SN: Perfusion MDCT enables early detection of therapeutic response to antiangiogenic therapy. AJR Am J Roentgenol 191: 133-139, 2008.
31. Galli R, Binda E, Orfanelli U, Cipelletti B, Gritti A, De Vitis S, Fiocco R, Foroni C, Dimeco F and Vescovi A: Isolation and characterization of tumorigenic, stem-like neural precursors from human glioblastoma. Cancer Res 64: 7011-7021, 2004.
32. Bao S, Wu Q, McLendon RE, Hao Y, Shi Q, Hjelmeland AB, Dewhirst MW, Bigner DD and Rich JN: Glioma stem cells promote radioresistance by preferential activation of the DNA damage response. Nature 444: 756-760, 2006.
33. Chung AS, Lee J and Ferrara N: Targeting the tumour vasculature: Insights from physiological angiogenesis. Nat Rev Cancer 10: 505-514, 2010.
34. Ferrara N: Role of vascular endothelial growth factor in physiologic and pathologic angiogenesis: Therapeutic implications. Semin Oncol 29 (6 Suppl 16): S10-S14, 2002.
35. Wang ES, Teruya-Feldstein J, Wu Y, Zhu Z, Hicklin DJ and Moore MA: Targeting autocrine and paracrine VEGF receptor pathways inhibits human lymphoma xenografts in vivo. Blood 104: 2893-2902, 2004.
36. Karp JE, Gojo I, Pili R, Gocke CD, Greer J, Guo C, Qian D, Morris L, Tidwell M, Chen H and Zwiebel J: Targeting vascular endothelial growth factor for relapsed and refractory adult acute myelogenous leukemias: Therapy with sequential 1-beta-d-arabinofuranosylcytosine, mitoxantrone, and bevacizumab. Clin Cancer Res 10: 3577-3585, 2004.
37. Qi L, Robinson WA, Brady BM and Glode LM: Migration and invasion of human prostate cancer cells is related to expression of VEGF and its receptors. Anticancer Res 23: 3917-3922, 2003.
38. Bates RC, Goldsmith JD, Bachelder RE, Brown C, Shibuya M, Oettgen P and Mercurio AM: Flt-1-dependent survival characterizes the epithelial-mesenchymal transition of colonic organoids. Curr Biol 13: 1721-1727, 2003.
39. Das B, Yeger H, Tsuchida R, Torkin R, Gee MF, Thorner PS, Shibuya M, Malkin D and Baruchel S: A hypoxia-driven vascular endothelial growth factor/Flt1 autocrine loop interacts with hypoxia-inducible factor-1alpha through mitogen-activated protein kinase/extracellular signal-regulated kinase 1/2 pathway in neuroblastoma. Cancer Res 65: 7267-7275, 2005.
40. Steiner HH, Karcher S, Mueller MM, Nalbantis E, Kunze S and Herold-Mende C: Autocrine pathways of the vascular endothelial growth factor (VEGF) in glioblastoma multiforme: Clinical relevance of radiation-induced increase of VEGF levels. J Neurooncol 66: 129-138, 2004.
41. Bachelder RE, Crago A, Chung J, Wendt MA, Shaw LM, Robinson G and Mercurio AM: Vascular endothelial growth factor is an autocrine survival factor for neuropilin-expressing breast carcinoma cells. Cancer Res 61: 5736-5740, 2001.
42. Broholm H and Laursen H: Vascular endothelial growth factor (VEGF) receptor neuropilin-1's distribution in astrocytic tumors. APMIS 112: 257-263, 2004.
43. Gray MJ, Wey JS, Belcheva A, McCarty MF, Trevino JG, Evans DB, Ellis LM and Gallick GE: Neuropilin-1 suppresses tumorigenic properties in a human pancreatic adenocarcinoma cell line lacking neuropilin-1 coreceptors. Cancer Res 65: 3664-3670, 2005.
44. Pan Q, Chanthery Y, Liang WC, Stawicki S, Mak J, Rathore N, Tong RK, Kowalski J, Yee SF, Pacheco G, *et al*: Blocking neuropilin-1 function has an additive effect with anti-VEGF to inhibit tumor growth. Cancer Cell 11: 53-67, 2007.
45. Kamiya T, Kawakami T, Abe Y, Nishi M, Onoda N, Miyazaki N, Oida Y, Yamazaki H, Ueyama Y and Nakamura M: The preserved expression of neuropilin (NRP) 1 contributes to a better prognosis in colon cancer. Oncol Rep 15: 369-373, 2006.
46. Hong X, Jiang F, Kalkanis SN, Zhang ZG, Zhang X, Zheng X, Mikkelsen T, Jiang H and Chopp M: Decrease of endogenous vascular endothelial growth factor may not affect glioma cell proliferation and invasion. J Exp Ther Oncol 6: 219-229, 2007.
47. Jia H, Bagherzadeh A, Hartzoulakis B, Jarvis A, Löhr M, Shaikh S, Aqil R, Cheng L, Tickner M, Esposito D, *et al*: Characterization of a bicyclic peptide neuropilin-1 (NP-1) antagonist (EG3287) reveals importance of vascular endothelial growth factor exon 8 for NP-1 binding and role of NP-1 in KDR signaling. J Biol Chem 281: 13493-13502, 2006.
48. Swendeman S, Mendelson K, Weskamp G, Horiuchi K, Deutsch U, Scherle P, Hooper A, Rafii S and Blobel CP: VEGF-A stimulates ADAM17-dependent shedding of VEGFR2 and crosstalk between VEGFR2 and ERK signaling. Circ Res 103: 916-918, 2008.
49. Lu Y, Xiang H, Liu P, Tong RR, Watts RJ, Koch AW, Sandoval WN, Damico LA, Wong WL and Meng YG: Identification of circulating neuropilin-1 and dose-dependent elevation following anti-neuropilin-1 antibody administration. MAbs 1: 364-369, 2009.
50. Gagnon ML, Bielenberg DR, Gechtman Z, Miao HQ, Takashima S, Soker S and Klagsbrun M: Identification of a natural soluble neuropilin-1 that binds vascular endothelial growth factor: In vivo expression and antitumor activity. Proc Natl Acad Sci USA 97: 2573-2578, 2000.